Acta Cryst. (1998). A**54**, 203–213

X-ray Standing Waves in Distorted Crystals

NORIO KATO

S 512 Hoshigaoka Iris, Meito-honmachi, Meito-ku, Nagoya 465, Japan

(*Received 3 February 1997; accepted 25 September 1997*)

Abstract

X-ray standing waves (SW) formed by dynamical diffraction are discussed analytically in the case of distorted crystals, in which the lattice has a monotonous elongation (or contraction) normal to the crystal surface. Both the external and the internal SWs are dealt with. Also, for the purpose of applications to standing-wave methods, the fluorescence yields of adsorbed atoms and impurities in the host crystal are formulated as a function of the off-Bragg angle of the incident beam. Through some numerical examples for special distortions, it is demonstrated that the conventional analysis based on the assumption of a perfect crystal may give serious errors (10–20%) on the location of foreign atoms, even when the deformation is so small that it is hardly detected by the rocking curve of the Bragg reflection.

1. Introduction

The X-ray standing waves (SW) formed by dynamical wave fields in perfect crystals was first studied by Batterman (1961, 1964). Later, it was demonstrated that the SW (henceforth called the internal SW) could be employed to determine the location of impurities in the crystal lattice (Batterman, 1969; Golovchenko *et al.*, 1974). The principle is to measure a rocking curve of the fluorescence (RCF) scattered from impurities due to the internal SW and to find a suitable model for the impurity location which fits the RCF.

Anderson, Golovchenko & Mair (1976) showed that the external SW could also be used to study adsorbed atoms on a crystal surface. The method is now one of the most common tools for surface crystallography.

However, in almost all works (*cf.* Hertel *et al.*, 1985; the reviews of Patel, 1996, and of Lagomarsino, 1996), the host crystals are assumed to be perfect and therefore Laue's dynamical theory of diffraction (*cf.* Zachariasen, 1945) is used as the theoretical basis. Remembering that dynamical waves are very sensitive to any lattice distortion (*cf.* Kato, 1974), the present situation is not satisfactory, at least in applying SW methods to precise structural research. The SW in distorted crystals is seriously discussed, probably for the first time, by Authier *et al.* (1989), which is a computer experiment on this subject. They used the algorithm of Bensoussan *et al.* (1987) to calculate the dynamical waves in distorted crystals. They, however, are concerned with the internal SW and the cases when the rocking curves of the Bragg reflection are significantly different from those of perfect crystals.

In the present paper, it is intended to elucidate how the SW is affected by continuous lattice distortions through an analytical approach. For quantitative analysis, we shall take up a class of lattice distortions for which the exact solutions of the wave fields are available (Kato, 1990, 1992*b*; henceforth referred to as P1 and P2, respectively). In this sense, the present paper constitutes a series with P1 and P2.

In the next section, some theoretical results for perfect crystals are summarized. In §3, the case of distorted crystals is discussed. Both the internal and external SWs are dealt with. Finally, the exact expressions for RCFs are obtained under a few limited conditions. In §4, some numerical examples are presented to demonstrate how RCFs are different from those of the perfect crystal even when the distortion is very weak. The final chapter is devoted to some conclusive remarks on SW methods.

2. Perfect crystals

2.1. *Standing waves and the Bragg-reflected intensity*

In the conventional theory, it is assumed that the crystal is ideally perfect and a plane wave impinges on a practically infinite surface. Then, in the two-beam case, the wave fields have the following forms.

External wave:

$$\mathbf{E}(\mathbf{r}) = \mathbf{E}_o \exp[i(\mathbf{K}_o \cdot \mathbf{r})] + \mathbf{E}_g \exp[i(\mathbf{K}_g \cdot \mathbf{r})]. \quad (1a)$$

Internal wave:

$$\mathbf{d}(\mathbf{r}) = \mathbf{d}_o \exp[i(\mathbf{k}_o \cdot \mathbf{r})] + \mathbf{d}_g \exp[i(\mathbf{k}_g \cdot \mathbf{r})], \quad (1b)$$

with the constraint

$$\mathbf{k}_g = \mathbf{k}_o + 2\pi\bar{\mathbf{g}}, \quad (2)$$

where $\bar{\mathbf{g}}$ is the reflection vector, which is assumed outwardly normal (x direction) to the crystal surface. Here, $\mathbf{E}$ and $\mathbf{d}$ represent the amplitude of the relevant waves, and $\mathbf{K}$ and $\mathbf{k}$ are their wave vectors. The suffices o and g denote the incident (transmitted) and the Bragg-reflected waves, respectively. For simplicity, henceforth,

we shall consider separately the σ and π components of the wave field so that they can be treated as scalar fields.

Owing to the boundary conditions on the crystal surface, it follows that

$$d_o = E_o \exp i\varphi_o, \tag{3a}$$

$$d_g = E_g \exp i\varphi_g, \tag{3b}$$

where

$$\varphi_o = [(\mathbf{K}_o - \mathbf{k}_o)\cdot \mathbf{r}_e], \tag{4a}$$

$$\varphi_g = [(\mathbf{K}_g - \mathbf{k}_g)\cdot \mathbf{r}_e]. \tag{4b}$$

Here $\mathbf{r}_e$ is an arbitrary position vector on the crystal surface and the celebrated tangential continuity of the wave vectors is satisfied. The wave vectors $\mathbf{k}_o$ and $\mathbf{k}_g$ are generally complex [see (12) and (13)], but the imaginary parts of φ_o and φ_g are identical. From (4), one obtains

$$\varphi_o - \varphi_g = 2\pi\{(\bar{\mathbf{g}}\cdot \mathbf{r}_e) - (\mathbf{G}\cdot \mathbf{r}_e)\}, \tag{4c}$$

where

$$2\pi\mathbf{G} = \mathbf{K}_g - \mathbf{K}_o. \tag{5}$$

If we write the amplitude ratio of the internal wave as

$$C \equiv (d_g/d_o) = |C|\exp(i\phi), \tag{6a}$$

it turns out from (3a) and (3b) that the amplitude ratio of the external wave is given by

$$E_g/E_o = |C|\exp[i(\varphi_o - \varphi_g + \phi)]. \tag{6b}$$

Consequently, (1a) gives the expressions for the external SW in the form

$$\begin{aligned} I_{\mathrm{ex}}(\mathbf{r}) &\equiv |E/E_o|^2 \\ &= 1 + |C|^2 + 2|C|\cos\{2\pi[\mathbf{G}\cdot(\mathbf{r} - \mathbf{r}_e)] \\ &\quad + 2\pi(\bar{\mathbf{g}}\cdot \mathbf{r}_e) + \phi\}. \end{aligned} \tag{7a}$$

Similarly, for the internal SW, (1b) gives

$$\begin{aligned} I_{\mathrm{in}}(\mathbf{r}) &\equiv |d/E_o|^2 \\ &= \{1 + |C|^2 + 2|C|\cos[2\pi(\bar{\mathbf{g}}\cdot \mathbf{r}) + \phi]\} \\ &\quad \times \exp[2\Delta\mathbf{k}''\cdot(\mathbf{r} - \mathbf{r}_e)], \end{aligned} \tag{7b}$$

where $\Delta\mathbf{k}''$ is the imaginary part of $\Delta\mathbf{k}$, which will be explained later [*cf.* (13)]. One can easily see that I_{in} is identical to I_{ex} on the crystal surface as it should be. In general, the spacing of the external SW is slightly different from that of I_{in}, which is always the lattice spacing d in the case of perfect crystals.

From (6b), the Bragg-reflected intensity (reflectivity) is given by

$$R = |E_g/E_o|^2 = |C|^2. \tag{8}$$

In many papers, $|C|$ in (7a) and (7b) is replaced by the square root of the reflectivity, $R^{1/2}$. The expressions are useful because R is a directly measurable quantity.

2.2. *The wave vectors*

In the following two sections, a glossary of symbols and some useful results of the dynamical theory are summarized.

The vacuum wave vectors are written in the form

$$\mathbf{K}_o = \bar{\mathbf{K}}_o - \Delta\mathbf{K}_o, \tag{9a}$$

$$\mathbf{K}_g = \bar{\mathbf{K}}_g - \Delta\mathbf{K}_g, \tag{9b}$$

where $\bar{\mathbf{K}}_o$ and $\bar{\mathbf{K}}_g$ are the wave vectors satisfying the exact Bragg condition, namely $\bar{\mathbf{K}}_g = \bar{\mathbf{K}}_o + 2\pi\bar{\mathbf{g}}$. The deviation vectors are given by

$$\Delta\mathbf{K}_o = (T, T/c), \tag{10a}$$

$$\Delta\mathbf{K}_g = (T, -T/c), \tag{10b}$$

where c denotes $\tan\theta_B$ and the tangential component T is given by

$$T = K\sin\theta_B\Delta\theta, \quad \Delta\theta = \theta - \theta_B. \tag{11a, b}$$

(Here, the symbol T is used instead of E in P1 and P2.)

Similarly to (9), the crystal wave vectors are written in the form

$$\mathbf{k}_o = \bar{\mathbf{K}}_o - \Delta\mathbf{k}, \tag{12a}$$

$$\mathbf{k}_g = \bar{\mathbf{K}}_g - \Delta\mathbf{k}, \tag{12b}$$

which are consistent with the constraint (2). The dynamical theory gives the result

$$\Delta\mathbf{k} = [T, \pm(\varepsilon^2 - M^2)^{1/2}/c], \tag{13}$$

where

$$\varepsilon = T - (1/2)\tau_c + (i/2)\mu_c, \tag{14}$$

$$M = (1/2)KP(\chi_g\chi_{-g})^{1/2}/\cos\theta_B = |M|\exp(i\Phi/2). \tag{15}$$

The physical meaning of the double sign in (13) will be explained later. In (15), P is the polarization factor of X-rays and $\{\chi_g\}$ are the Fourier coefficients of the complex polarizability ($\chi = \chi' + i\chi''$) of the crystal. In addition,

$$\tau_c = K(-\chi_o')/\cos\theta_B \quad (>0), \tag{16a}$$

$$\mu_c = K(\chi_o'')/\cos\theta_B \quad (>0), \tag{16b}$$

$$\Phi = \arg[\chi_g\chi_{-g}], \tag{17}$$

where $\mu_c\cos\theta_B$ is the linear absorption coefficient and arg[...] implies the phase of [...].

2.3. *The amplitude ratio*

According to the dynamical theory,

$$C = (\chi_g/\chi_{-g})^{1/2} M^{-1}\{-\varepsilon + (\varepsilon^2 - M^2)^{1/2}\}. \quad (18)$$

As a consequence, the phase angle ϕ in (6*a*) and (6*b*) is given by

$$\phi = (1/2)(\Phi_g - \Phi) + \phi_o, \quad (19)$$

where

$$\Phi_g = \arg[\chi_g/\chi_{-g}], \quad (20a)$$

$$\phi_o = \arg[-\varepsilon + (\varepsilon^2 - M^2)^{1/2}]. \quad (20b)$$

Notice that ϕ_o depends on the deviation angle $\Delta\theta$ and the phases Φ and Φ_g are intrinsic to the crystal concerned.

Incidentally, the deviation parameter η used in many articles (*e.g.* Batterman, 1964; Patel, 1996) is $(-\varepsilon/M)$ in the present notations. Also, the factor $(\chi_g/\chi_{-g})^{1/2}$ in (18) is often omitted. It is, however, important in polar crystals.

In non-absorbing crystals, ε and M are real, so that ϕ_o changes from 0 to π as the ε value increases from $-|M|$ to $|M|$. In absorbing crystals, the analytical expressions for ϕ_o in terms of real quantities are rather complicated. However, the numerical evaluation is not made more difficult by using the complex expression (20*b*) as it is (see Kato, 1992*a*).

Here we shall comment on the double sign of (13). According to mathematical convention, the imaginary part of $(\varepsilon^2 - M^2)^{1/2}$ is fixed to be positive. Physically, however, $(\Delta\mathbf{k})_x$ can take both signs as indicated there. Nevertheless, in considering sufficiently thick crystals (*i.e.* the Darwin–Prins case), only the damping solution along the $-x$ direction is permissible so that only the + sign must be retained both in (13) and in (18). In very thin crystals, Ewald's solution must be used. In this case, the wave field is composed of two waves specified by + and − signs, so that the SWs are not simple as in (7*a*) and (7*b*). We shall not discuss such a special case in this paper.

From the expressions (7*a*) and (7*b*), one can calculate RCFs. However, to avoid duplication, we shall postpone the subject until §3.5 in which the distorted crystal is discussed. The RCF for perfect crystals can be given as a special case.

3. Distorted crystals

3.1. *A few remarks on the lattice distortion*

In distorted crystals, the (local) reflection vector $\mathbf{g}$ is no longer constant and has the form (*cf.* Kato, 1974)

$$\mathbf{g} = \bar{\mathbf{g}} - \mathrm{grad}[\bar{\mathbf{g}} \cdot \mathbf{u}(\mathbf{r})], \quad (21)$$

where $\bar{\mathbf{g}}$ is the reflection vector of a perfect crystal and $\mathbf{u}$ is the displacement vector of the lattice point when the crystal is deformed. Henceforth,

$$\varphi = 2\pi(\bar{\mathbf{g}} \cdot \mathbf{u}) \quad (22)$$

is called the lattice phase.

As mentioned in the *Introduction*, we shall take up a class of lattice distortions, namely an elongation (or contraction) normal to the crystal surface, which is written in the form

$$(-\Delta\mathbf{g})_x \equiv \mathrm{grad}_x(\varphi/2\pi) = (\pi c)^{-1} D_o \tanh(\alpha x), \quad (23)$$

where D_o and α are parameters to specify the magnitude and steepness of the deformation, respectively. The model of the distortion is schematically illustrated in Fig. 1. By integrating (23), one obtains

$$\varphi = (2D_o/\alpha c)\log(\cosh \alpha x), \quad (24)$$

where the integral constant $\varphi(0)$ is assumed to be zero.

Another remark must be made on the distorted net plane. It can be defined by the integral form of (21), *i.e.*

$$\int_0^{\hat{\mathbf{r}}} (\mathbf{g} \cdot \mathrm{d}\mathbf{r}) = (\bar{\mathbf{g}} \cdot \hat{\mathbf{r}}) - \varphi(\hat{\mathbf{r}})/2\pi = m. \quad (25)$$

In general, this defines a set of discrete surfaces, each being specified by integer m. In our model, they are a set of planes parallel to the crystal surface. In this case, $\bar{\mathbf{g}} \cdot \hat{\mathbf{r}}$ can be replaced by $\hat{x}/d$.

3.2. *The amplitude ratio*

The external wave field can be written as (1*a*) even when the crystal is deformed, and the amplitudes (E_o, E_g) are constant because E is a vacuum wave. For the internal field, unlike the case of perfect crystals, one cannot define explicitly the wave vectors $\mathbf{k}_o$ and $\mathbf{k}_g$ [equations

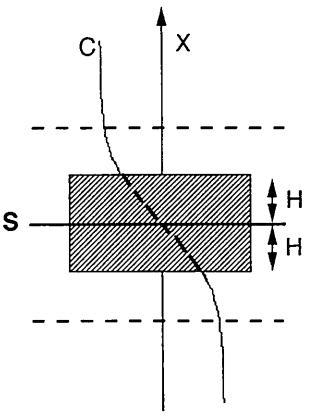

Fig. 1. Schematic illustration of the lattice distortion. *X*: The coordinate axis normal to the net plane, the origin being fixed in space. *H*: The half thickness of the deformed area [see equation (50*c*)]. Curve *C*: The deviation of the reflection vector $(\Delta\mathbf{g})_x$ [see equation (23)]. *S*: The crystal surface parallel to the net plane. In general, it may be located at any position as shown by broken lines. The position is specified by X_e.

(2), (12*a*) and (12*b*)]. For this reason, the internal wave is written for convenience in the form

$$\mathrm{d}(\mathbf{r}) = d_o \exp[i(\bar{\mathbf{K}}_o \cdot \mathbf{r})] + d_g \exp[i(\bar{\mathbf{K}}_g \cdot \mathbf{r})] \qquad (26)$$

and (d_o, d_g) are regarded as spatial functions in the crystal. Also, for a purely mathematical reason, we shall use

$$u(t,x) = \exp(-i\varphi/2)d_o(\mathbf{r}) \qquad [\mathrm{P1.2.3}a] \quad (27a)$$

$$v(t,x) = \exp(i\varphi/2)d_g(\mathbf{r}) \qquad [\mathrm{P1.2.3}b] \quad (27b)$$

instead of (d_o, d_g). The equation number in square brackets refers to the equation in previous papers. The coordinate t is the tangential component of $\mathbf{r}$ in the plane of incidence, although it is often suppressed. In the present model of the lattice distortion, the functions (u, v) satisfy an ordinary differential equation of second order [P1.2.9], which is derived from a set of partial differential equations of Takagi–Taupin type. Therefore, (u, v) have two linearly independent solutions in general, which are called types (*a*) and (*b*). They attenuate along $-x$ and $+x$ directions, respectively. For the same reason that we use to adopt the + sign in (18), only a set of solutions of type (*a*) is physically permissible. We shall write them as (u_a, v_a).

The boundary conditions on the crystal surface ($x = x_e$) can be written explicitly [*cf.* equations (1*a*), (9*a*), (9*b*), (26), (27*a*) and (27*b*)] as

$$E_o \exp[-i(\Delta\mathbf{K}_o \cdot \mathbf{r}_e)] = u_a(x_e)\exp[i\varphi(x_e)/2], \qquad (28a)$$

$$E_g \exp[-i(\Delta\mathbf{K}_g \cdot \mathbf{r}_e)] = v_a(x_e)\exp[-i\varphi(x_e)/2]. \qquad (28b)$$

From these, the amplitude ratio of the external waves is given by

$$C_{\mathrm{ex}} \equiv E_g/E_o = [v_a(x_e)/u_a(x_e)]\exp\{-i[\varphi(x_e) + \psi(x_e)]\}, \qquad (29)$$

where

$$\psi = [(\Delta\mathbf{K}_o - \Delta\mathbf{K}_g) \cdot \mathbf{r}_e]. \qquad (30)$$

Inside the crystal, the amplitude ratio is a function of x. Meanwhile, we shall write it in a similar manner to (29):

$$C_{\mathrm{in}} \equiv d_g/d_o = [v_a(x)/u_a(x)]\exp[-i\varphi(x)]. \qquad (31)$$

3.3. *The solutions of $u_a(x)$ and $v_a(x)$*

In this section, a glossary of notations is listed. The details are explained in the previous papers, P1 and P2.

$$\bar{\nu} = D_o/\alpha c, \qquad [\mathrm{P2.2.19}] \qquad (32)$$

$$p + q = -i[(\varepsilon - D_o)^2 - M^2]^{1/2}/\alpha c, \qquad [\mathrm{P2.2.20}a] \qquad (33a)$$

$$p - q = -i[(\varepsilon + D_o)^2 - M^2]^{1/2}/\alpha c, \qquad [\mathrm{P2.2.20}b] \qquad (33b)$$

$$a = -i\bar{\nu} + q, \quad b = 1 + i\bar{\nu} + q, \quad c' = 1 + q - p. \qquad [\mathrm{P1.4.12}] \quad (34a, b, c)$$

The last three† are the parameters to specify the standard hypergeometric function $F(a, b; c'; z)$. (See, for example, Bateman-Eredelyi, 1953; Abramowitz & Stegun, 1964.)

In order to specify the position, we often use the variable ξ instead of x. It is defined by

$$\xi = \tanh \alpha x \quad (\alpha > 0). \qquad [\mathrm{P1.3.6}a] \quad (35)$$

With the use of these notations, the wavefields $u_a(x)$ and $v_a(x)$ can be written as follows:

$$u_a(x) = G(\xi)F[-i\bar{\nu} + q, 1 + i\bar{\nu} + q; 1 + p + q; (1 + \xi)/2], \qquad [\mathrm{P1.4.13}b] \quad (36a)$$

$$v_a(x) = C_a G(\xi)F[i\bar{\nu} + q, 1 - i\bar{\nu} + q; 1 + p + q; (1 + \xi)/2], \qquad [\mathrm{P1.4.16}] \quad (36b)$$

where

$$G(\xi) = (\cosh \alpha x)^{-q} \exp(p\alpha x), \qquad [\mathrm{P1.4.21}a] \quad (37)$$

$$C_a = (\chi_g/\chi_{-g})^{1/2} M^{-1}\{-(\varepsilon - D_o) + [(\varepsilon - D_o)^2 - M^2]^{1/2}\}. \qquad [\mathrm{P2.2.23}b] \quad (38)$$

Here, C_a is the amplitude ratio for a perfect crystal corresponding to the region of $x = -\infty$ in the present model of distortion.

Using the results (36*a*) and (36*b*), we obtain the ratio (v_a/u_a) in the form

$$C_d(\xi) \equiv v_a/u_a = C_a \frac{F[i\bar{\nu} + q, 1 - i\bar{\nu} + q; 1 + p + q; (1 + \xi)/2]}{F[-i\bar{\nu} + q, 1 + i\bar{\nu} + q; 1 + p + q; (1 + \xi)/2]}. \qquad (39)$$

3.4. *The standing wave and the rocking curve*

Now, one can write the external SW in parallel with the expression (7*a*) in the case of perfect crystals. A modification, however, is required not only to replace E_g/E_o by C_{ex} [equation (29)] but also to express C_{ex} in terms of the calculable amplitude ratio

$$C_d(\xi) = |C_d| \exp(i\delta). \qquad (40)$$

Here, from (39), the phase angle is given by

$$\delta(\xi) = \tfrac{1}{2}(\Phi_g - \Phi) + \delta_0 + \delta_1(\xi) - \delta_2(\xi), \qquad (41a)$$

where

$$\delta_0 = \arg\{-(\varepsilon - D_o) + [(\varepsilon - D_o)^2 - M^2]^{1/2}\} \qquad (41b)$$

† To avoid confusion with $c = \tan\theta_B$, c' is used for c in the standard textbooks.

and δ_1 and δ_2 are the phase angles of the hypergeometric functions in the numerator and the denominator, respectively. Notice that δ_0 is independent of $\xi(x)$ but depends on the off-Bragg angle $\Delta\theta$. On the other hand, δ_1 and δ_2 depend on the two variables.

Obviously, $|C_{ex}| = |C_d(\xi_e)|$. Although $\bar{\mathbf{g}}$ is defined as the reflection vector of the undistorted crystal, the geometrical relation

$$2\pi\bar{\mathbf{g}} = \bar{\mathbf{K}}_g - \bar{\mathbf{K}}_o = 2\pi\mathbf{G} + \Delta\mathbf{K}_g - \Delta\mathbf{K}_o$$

does hold also in the case of distorted crystals. Therefore, (30) can be rewritten as

$$\psi = 2\pi\{(\mathbf{G}\cdot\mathbf{r}_e) - (\bar{\mathbf{g}}\cdot\mathbf{r}_e)\}. \tag{42}$$

According to these preliminary arguments, one can write the external SW in the form

$$\begin{aligned} I_{ex}(\mathbf{r}) &\equiv |E/E_o|^2 \\ &= 1 + |C_d(\xi_e)|^2 + 2|C_d(\xi_e)| \\ &\quad\times\cos\{2\pi[\mathbf{G}\cdot(\mathbf{r}-\mathbf{r}_e)] + \delta(\xi_e) - \varphi(x_e) \\ &\quad + 2\pi(\bar{\mathbf{g}}\cdot\mathbf{r}_e)\}, \end{aligned} \tag{43}$$

in which ξ_e is the value of ξ on the crystal surface.

Similarly, remembering that $d_g/d_o = |C_d|\exp[i(\delta-\varphi)]$ from (31), (39) and (40) and $|E_o| = |u_a(x_e)|$ from (28*a*), one can obtain the expression for the internal SW in the form

$$\begin{aligned} I_{in}(\mathbf{r}) &\equiv |d/E_o|^2 \\ &= \{1 + |C_d(\xi)|^2 + 2|C_d(\xi)| \\ &\quad\times\cos[2\pi(\bar{\mathbf{g}}\cdot\mathbf{r}) + \delta(x) - \varphi(x)]\} \\ &\quad\times|u_a(x)/u_a(x_e)|^2. \end{aligned} \tag{44}$$

Again, one can see that $I_{ex} = I_{in}$ on the crystal surface, $\mathbf{r} = \mathbf{r}_e$.

The rocking curve (reflectivity) can be given straightforwardly by

$$R = |C_d(\xi_e)|^2. \tag{45}$$

As for the case of perfect crystals, $|C_d(\xi_e)|$ in (43) can be replaced by $R^{1/2}$.

3.5. *The rocking curve for fluorescence (RCF)*

First, the fluorescence due to the external SW is discussed. In general, the fluorescence yield is given by

$$Y_{ex} = \int \rho_f(\mathbf{r}) I_{ex}(\mathbf{r})\,d\mathbf{r}, \tag{46a}$$

where $\rho_f(\mathbf{r})$ is a distribution function for the scattering body. Here, for simplicity, it is assumed that all adsorbed atoms are located at equivalent positions $\mathbf{r}_a$ with respect to the crystal surface and ρ_f of a single atom has the form of $\sigma_a\delta(\mathbf{r}-\mathbf{r}_a)$, where σ_a is the cross section of fluorescence scattering. The elaboration of this model may not be difficult but is out of the scope of the present paper. Thus, (46*a*) can be simplified as

$$Y_{ex}(\Delta\theta) = N_a\sigma_a I_{ex}(\mathbf{r}_a), \tag{46b}$$

where N_a is the number of scattering atoms and I_{ex} is given by (43). [Equation (7*a*) may be used for perfect crystals.] Through $|C_d|$, $\mathbf{G}$ and the phases, Y_{ex} is a function of $\Delta\theta$.† It is called the rocking curve for fluorescence (RCF) in this paper. Notice that, if one takes a lattice net plane for the crystal surface, the term $2\pi(\bar{\mathbf{g}}\cdot\mathbf{r}_e) - \varphi(x_e)$ can be dropped in the expression of I_{ex} by virtue of (25).

Next, we shall consider a RCF of impurities due to the internal SW. Here, all impurities in the host crystal must be taken into account. However, it is assumed that all impurities have a fixed relation to the deformed net plane. Under these circumstances, conveniently, $\mathbf{r}_i$ can be written as $\mathbf{r}_i^m + \hat{\mathbf{r}}_m$, where $\hat{\mathbf{r}}_m$ is the position vector for the mth net plane, and $\mathbf{r}_i^m$ is the relative vector from this net plane. Then, the RCF of impurity atoms is given by

$$Y_{in}(\Delta\theta) = N_i\sigma_i\sum_m I_{in}(\mathbf{r}_i^m + \hat{\mathbf{r}}_m)A_f(\mathbf{r}_i^m + \hat{\mathbf{r}}_m), \tag{47}$$

where the suffix i is used for the impurity atom and N_i is the number of impurities associated with one net plane. Here, they are assumed to be independent of the index m. In some problems, the impurity distribution in the host crystal may be important. Then, the factor N_i must be put inside the summation the same as N_m. One needs the factor A_f, which accounts for the attenuation of the fluorescence X-rays coming out of the crystal. However, the details of this subject are not discussed here (see §4.3).

The functional form of I_{in} is given by (44) ($\mathbf{r}_i = \mathbf{r}_i^m + \hat{\mathbf{r}}_m$). Again, by virtue of (25), one can rewrite $2\pi(\bar{\mathbf{g}}\cdot\hat{\mathbf{r}}_m)$ as $\varphi(\hat{x}_m)$. In order to emphasize that we are concerned with the impurities associated with the mth net plane, tentatively, the coordinate x is denoted by $x_{i,m}$. However, the difference between $x_{i,m}$ and $\hat{x}_m$ is less than the local lattice spacing and the functions φ, δ and u_a are practically unchanged within this distance. Therefore, to a good approximation, the argument $x_{i,m}$ can be replaced by $\hat{x}_m$ and the two φ terms cancel each other. Thus, it turns out that I_{in} has the following form:

$$\begin{aligned} I_{in}(\mathbf{r}_i^m + \hat{\mathbf{r}}_m) &= \{1 + |C_d(\hat{\xi}_m)|^2 \\ &\quad + 2|C_d(\hat{\xi}_m)|\cos[2\pi(\bar{\mathbf{g}}\cdot\mathbf{r}_i^m) + \delta(\hat{x}_m)]\} \\ &\quad\times|u_a(\hat{x}_m)/u_a(x_e)|^2, \end{aligned} \tag{48}$$

† From equations (2), (5), (9*a*) and (9*b*), one obtains the relation $2\pi\mathbf{G} = 2\pi\bar{\mathbf{g}} + \Delta\mathbf{K}_o - \Delta\mathbf{K}_g$. With the additional use of (10*a*), (10*b*), (11*a*) and (11*b*), this leads to the relation between $|\mathbf{G}|$ and $|\bar{\mathbf{g}}|$; *i.e.*

$$|G| = (1 + \Delta\theta/\tan\theta_g)|\bar{\mathbf{g}}|.$$

In most cases, however, the difference between $\mathbf{G}$ and $\bar{\mathbf{g}}$ can be neglected.

where $\hat{\xi}_m$ is the value of ξ on the mth net plane and $\bar{\mathbf{g}} \cdot \mathbf{r}_i^m$ is a constant in our model. With the same argument, $A_f(\mathbf{r}_i^m + \hat{\mathbf{r}}_m)$ can be written as $A_f(\hat{\mathbf{x}}_m)$.

For obtaining the yield numerically, (47) is inconvenient because the total number of net planes is enormous. Then, the summation is to be replaced by an integration with respect to x, set equal to $\hat{x}_m$. Since the number of net planes in dx is $|g(x)|\,dx$, we shall have

$$Y_{\text{in}}(\Delta\theta) = N_i\sigma_i \int_{-\infty}^{x_e} I_{\text{in}}(\mathbf{r}_i^m + \hat{\mathbf{r}}_m) A_f(x)|g|\,dx. \qquad (49)$$

4. Numerical examples

4.1. *Preliminaries*

We shall show some examples of RC, the phase of SW and RCF. For convenience, the following normalized parameters defined in paper P2 will be used. In the following, $\Lambda = c/|M|$ is a kind of extinction distance.

$X = x/\Lambda$: the coordinate normal to the crystal surface (50*a*)

$A = \mu_c\Lambda$: a parameter indicating absorption (50*b*)

$H = |M|/\alpha c = \Lambda_d/\Lambda$: the half thickness of deformed area (50*c*)

$T/|M|$: the off-Bragg angle referred to the crystal at $X = 0$ (50*d*)

Consequently, $(T - D_o)/|M|$ is the off-Bragg angle referred to the perfect crystal in the region of $X = -\infty$, which will often be called the 'bottom crystal'.

As discussed in P2, various rocking curves are expected depending on X_e, A and H. In the following, however, the range of parameters is confined such that the RC is similar to that of perfect crystals, because we are interested in such cases for most SW methods. Also, for simplicity, the parameters are fixed as $X_e = 0$, $D_o/|M| = 3$ and $\tau_c = 0$ in (14) unless otherwise stated. In addition, the constant phases, Φ and Φ_g, are omitted. The physical implications will be discussed in §5.

4.2. *RCF due to external SW*

4.2.1. *Non-absorbing crystals (A = 0).* In order to explain the underlying principles, first we shall consider this characteristic case. As discussed in P2, even if the crystal is distorted near the crystal surface, the RC has a region of total reflection corresponding to the bottom crystal. Fig. 2(*a*) is a set of RCs calculated by (45) and (39) for $H = 0.002$ (i), 0.02 (ii) and 0.2 (iii). The first two are indistinguishable from Darwin's top-hat curve with the center at $D_o/|M| = 3$, but case (iii) is slightly different from it in the tails of the RC. We shall regard case (i) as a perfect crystal. Incidentally, if (8) and (18) are used, the same RC is obtained except that the centre is shifted to $T/|M| = 0$.

Fig. 2(*b*) shows the phase δ of C_d [equation (41*a*)] for the above three cases. We notice that the phase is very sensitive to the lattice distortion. Fig. 2(*c*) illustrates RCFs in the respective cases calculated by (46*b*), omitting the constant factor $\sigma_a N_a$. Here, it is assumed

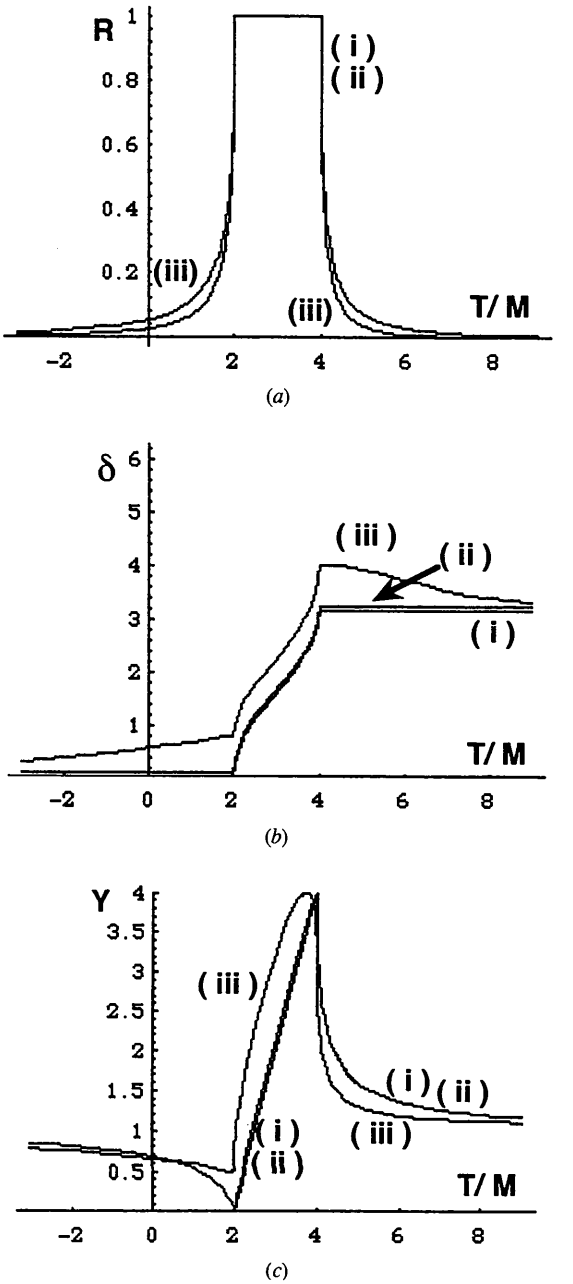

Fig. 2. The case of non-absorbing crystals ($A = 0$). (*a*), (*b*) and (*c*) are the reflectivity (R), the phase (δ) and the fluorescence yield (Y) due to the external SW, respectively. The parameters H used for the curves (i), (ii) and (iii) are 0.002, 0.02 and 0.2, respectively, and $L_a = \mathbf{G} \cdot (\mathbf{r}_a - \mathbf{r}_e) = 0.5$ is used for (*c*). The absolute symbol $|M|$ in the abscissa is suppressed, for convenience. The same convention is used in the following figures.

that $L_a = \mathbf{G} \cdot (\mathbf{r}_a - \mathbf{r}_e)$ of (43) is 0.5; *i.e.* the adsorbed atoms are located normally at the half spacing of the external SW from the crystal surface. Notice that the central part of (iii) is significantly different from that of the perfect crystal (i).

4.2.2. *Absorbing crystals ($A = 0.1$).* The general behaviour is not very different from the case of non-absorbing crystals, except that the RC has a round shape (Darwin–Prins curve). As shown in Fig. 3(*a*), we notice that RCs of distorted crystals are practically the same as the perfect crystal (P) unless H is larger than 0.1. There, the curve for $H = 0.1$ is denoted by D. Again, since the phase δ is very sensitive to the distortion (physically speaking, the thickness of the distorted area), the RCFs corresponding to D and P are very different for the same value of L_a.

However, one can obtain nearly the same RCFs by adjusting the parameter L_a for perfect or distorted crystals. Fig. 3(*b*) is an example where the curve D' is obtained with $(L_a, H) = (0.50, 0.1)$ whereas the curve P' is the case of (0.58, 0.002). This example demonstrates

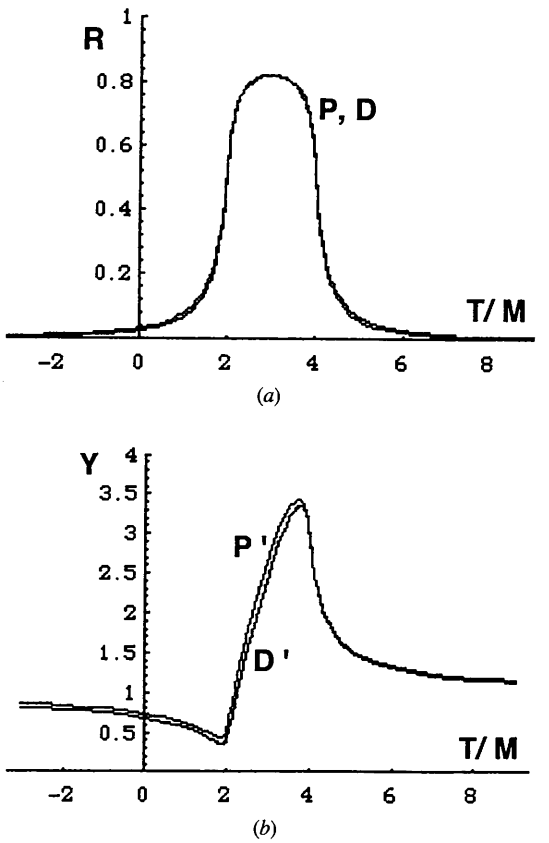

Fig. 3. The case of absorbing crystals ($A = 0.1$). (*a*) and (*b*) are the reflectivity and the fluorescence yield due to the external SW, respectively. The parameters for curves P (perfect crystal) and D (distorted crystal) in (*a*) are $H = 0.002$ and 0.1, respectively. The parameters for P' and D' in (*b*) are $(L_a, H) = (0.58, 0.002)$ and (0.50, 0.1), respectively. Notice that practically $P = D$ and $P' = D'$.

that if the crystal is distorted the conventional assumption of a perfect crystal leads to 16% error for the location of adsorbed atoms.

4.3. *RCF due to internal SW*

In this section, we shall discuss first SW and then RCF. The expression for SW [equation (48)] is a product of the interference factor $\{\ldots\}$ and the intensity factor $|\ldots|^2$. Since they are functions of the two variables $T/|M|$ and X, we explain them using contour diagrams. The parameters are fixed as $X_e = 0$, $A = 0.1$ and $L_i = (\bar{\mathbf{g}} \cdot \mathbf{r}_i^m) = 0.50$ throughout. The set of drawings in Fig. 4 shows the case of perfect crystals. The top and bottom curves illustrate the profiles of each contour diagram at $X = 0$ and -3.0, respectively. Obviously, the interference factor (*a*) is independent of the variable X because $\delta_1 = \delta_2 = 0$ in perfect crystals and the intensity profile is the same as the RCF due to the external SW given by (43) with $L_a = 0.5$. The intensity factor (*b*) indicates an attenuation of the intensity. The rapid attenuation in the central region ($2 < T/|M| < 4$) is due to well known extinction effects. Accordingly, the product (*c*), *i.e.* the SW profile, depends significantly on the depth of the crystal.

Fig. 5 shows similar diagrams for a deformed crystal ($H = 0.2$). The intensity profile at $X = 0$ in (*a*) is the same as the RCF due to the external SW in distorted crystals but the profile below $X \approx -0.5$ is nearly the same as that of the perfect crystal (Fig. 4*a*). The intensity factor (*b*) is essentially the same as that of the perfect crystal. As a result, the product (*c*) is similar to that of the perfect crystal except in the surface area above $X \approx -0.5$. However, detailed inspection shows that the intensity factor (*b*) is asymmetric with respect to $T/|M| = 3$. Accordingly, the SW profile is larger than the profile of the perfect crystal near $T/|M| \approx 4$.

Next, we shall discuss the RCF of the impurities, which can be calculated by (49). The expression for $A_f(x)$ depends on the experimental conditions to collect the fluorescence X-rays. Here, for simplicity, it is assumed that it is proportional to $\exp\{-B(X_e - X)\}$, where $B = \mu_f \Lambda / \cos\theta_B$ and μ_f is the linear absorption coefficient of the fluorescence X-rays. Notice that B must be larger than A because the energy of the fluorescence is smaller than that of the incident X-rays.

The series in Fig. 6 shows a comparison of RCFs for the perfect crystal ($H = 0.002$) and the distorted crystal ($H = 0.2$). Figs. 6(*a*), (*b*) and (*c*) correspond to the cases of $B = 0.3$, 3 and 10, respectively. Without detailed calculations, one can anticipate easily that, for smaller B, the RCFs for the perfect and distorted crystals are nearly the same because the main contribution comes from the bottom crystal. Only for larger B is the difference appreciable. The difference near $T/|M| \approx 4$ in every case is due to the asymmetry of the intensity factor (*b*) mentioned above.

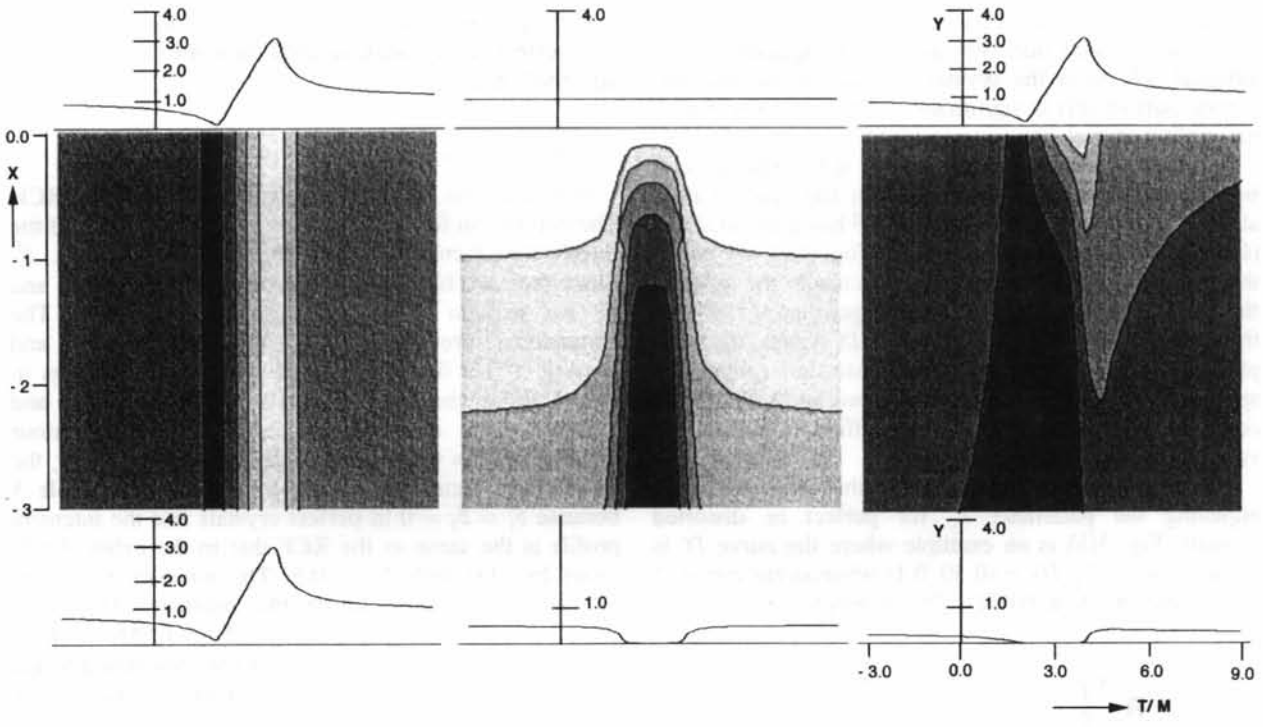

(a) (b) (c)

Fig. 4. The case of an absorbing perfect crystal ($A = 0.1$, $H \doteq 0.002$). The contour diagrams (*a*), (*b*) and (*c*) represent the interference factor, the intensity factor and the internal SW, respectively [see equation (48)]. $L_i = (\bar{\mathbf{g}} \cdot \mathbf{r}_i^m) = 0.5$ is used for (*a*) and (*c*). The top curves are the profiles at $X = 0$ and the bottom ones are the profiles at $X = -3.0$.

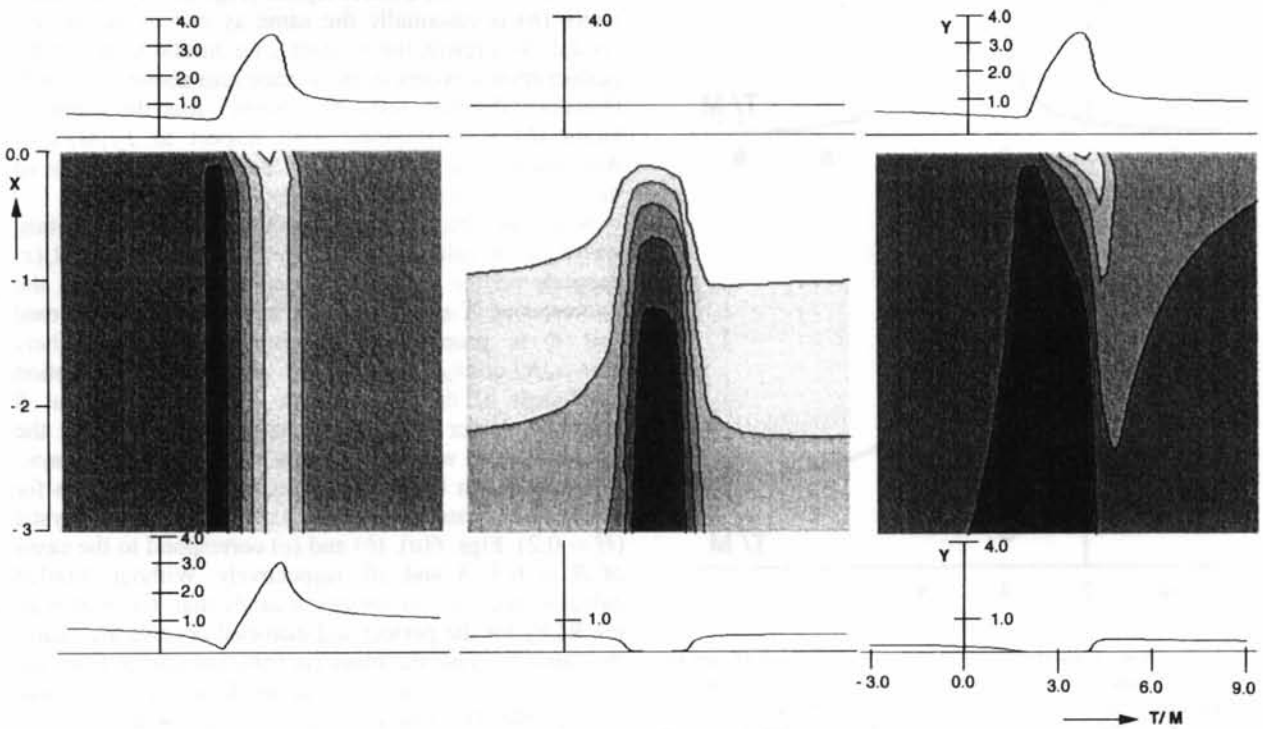

(a) (b) (c)

Fig. 5. Diagrams similar to Fig. 4 for an absorbing distorted crystal ($A = 0.1$, $H = 0.2$). $L_i = 0.5$ is used for (*a*) and (*c*).

All calculations were carried out by *Mathematica* Version 2 designed for PCs. In the present program, the graphical representations were directly connected with the basic formulae so that one could grasp easily their physical implications. Also, any intermediate stage of calculations could be checked. Fig. 2(*b*) to Fig. 2(*c*) is an example. The contour diagrams (*a*) and (*b*) help in understanding diagram (*c*) in Figs. 4 and 5. The computation time was less than 20 s for most 2D curves and about 20 min for the contour diagrams.

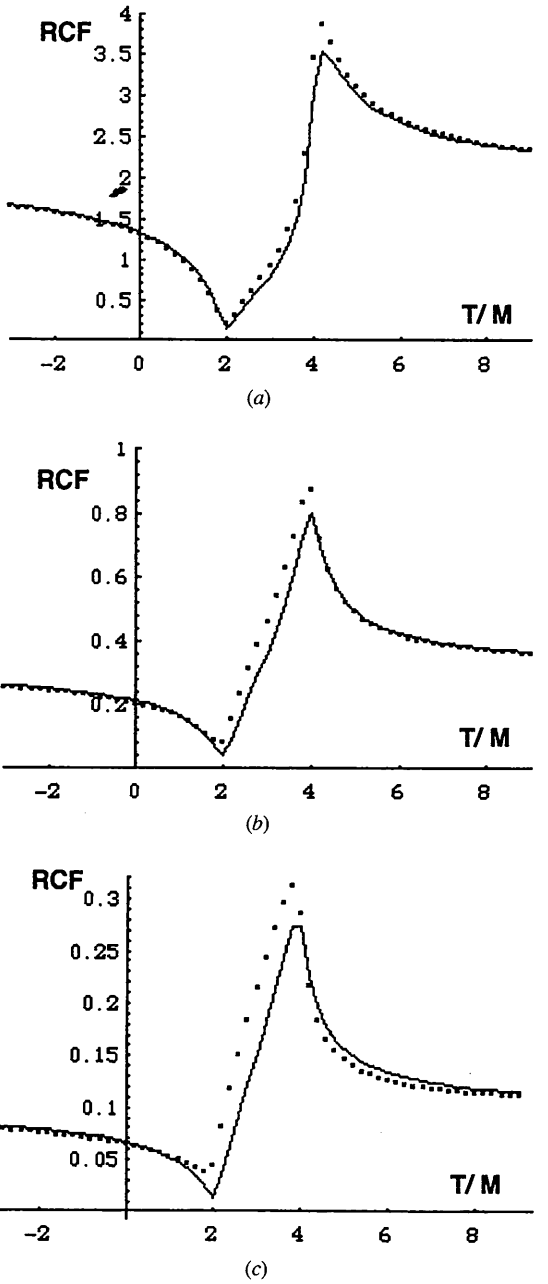

Fig. 6. RCFs due to the internal SW for various absorption coefficients of the fluorescence X-rays: $B = 0.3$ (*a*), 3.0 (*b*) and 10 (*c*). The continuous curves show the perfect crystal ($H = 0.002$) and the squares illustrate the case of the distorted crystal ($H = 0.2$). Throughout, $A = 0.1$ and $L_i = 0.5$ are used.

5. Discussion and conclusions

5.1. *Remarks on the present theory*

The basic diffraction theory is described in P1 and P2. From it, the analytical expressions of the RC (45) and the RCFs due to the external and the internal SWs [(46*b*) and (49), respectively] are derived for distorted crystals. The phase angles of E_g/E_o and d_g/d_o are exactly formulated because they are crucial to the positions of the SWs. Using these results, one can determine the positions of foreign atoms referred to the deformed net plane of the host crystal.

5.1.1. *The absolute position of the antinode (or node).* In the present theory, we are concerned with the location referred to the mth net plane rather than the absolute position in space. By using the same arguments to derive (48) from (44), the antinode position ($\mathbf{r}_z^m$) is given by

$$2\pi(\bar{\mathbf{g}} \cdot \mathbf{r}_z^m) = 2\pi x_z^m/\bar{d} = -\delta(\hat{x}_m) \qquad (51)$$

to a good approximation. The first two terms of (41*a*) for δ represent the phase in the case of the perfect bottom crystal and $\delta_1 - \delta_2$ is the deviation from it. Fig. 7 shows some examples of the deviation for various depths of the net plane ($-\hat{x}_m$). In general, it is large on the crystal surface and near the Bragg peak and it tends to zero with increasing $|\hat{x}_m|$ and $|\Delta\theta|$.

If we need the absolute position in space, it is easily obtained by adding the coordinate $\hat{x}_m$ of the mth net plane which is calculable by the use of the transcendental equation (25). Accordingly, the spacing of the internal SW is also a function of the off-Bragg angle and the depth.

5.1.2. *The lattice distortion.* The local reflection vector $\mathbf{g}(x)$ is schematically illustrated in Fig. 1. By changing the parameters, α, D_o and x_e, one can construct a model distortion, which changes monotonously under the constraint that $\mathbf{g}(x)$ has no tangential component. The surface fabrications in semiconductor devices may cause distortions of this type. In this paper, only the case of weak distortions was discussed. However, the present theory can be applied to the case of large distortions, for which the RC may have two peaks or oscillatory characters (Authier *et al.*, 1989; Kato, 1992*b*).

It must be noted here that we are concerned with only long-range distortions, which are averaged ones in a sense. When the displacement $\mathbf{u}(\mathbf{r})$ changes rapidly over an atomic scale as in dislocation cores and impurity clusters, and there are plenty of these defects, the present theoretical basis is doubtful. In such cases, we must start with a statistical theory of dynamical diffraction (*cf.* the review article of Kato, 1996) for obtaining the SW (intensity field) which creates the fluorescence X-rays.

5.1.3. *The phase angles intrinsic to the crystal.* In the numerical calculation (§4), Φ and Φ_g were dropped for simplicity. However, these phases are important in the practice of SW methods. As shown in (43) and (44), the constant phase $\frac{1}{2}(\Phi_g - \Phi)$ in the phase δ given by (41*a*) shifts the location of the internal and the external SW.

The phase Φ_g comes from the factor χ_g/χ_{-g} in the amplitude ratios, equations (18) and (38). This factor is omitted in many articles but is required for polar crystals. The phase Φ relates not only to the location of SW but also to the asymmetric profile of the RC. Because the lattice distortion also gives rise to the asymmetry as illustrated in Fig. 2(*a*), one must distinguish the two physical origins of the asymmetry. In other words, Φ cannot be used as a fitting parameter for describing the RC unless the crystal is assumed to be perfect.

5.2. *Remarks on SW methods*

First, we consider the external SW method. An important conclusion of the present work is to point out that the RCF is very sensitive to the lattice distortion if it extends over a tenth of Λ. The numerical examples of Fig. 3 illustrate that, even in the case of a weak distortion that is hardly detected by the RC, the best fitting value of L_a for the RCF is not unique, depending on the lattice distortion. This result is rather serious for the external SW method when it is applied to determining the position $\mathbf{r}_a$ of adsorbed atoms.

Next, we shall consider the internal SW method. When the absorption of the fluorescence X-rays is small, the RCF is nearly the same as that expected for the bottom crystal. Fig. 6(*a*) shows an example. Therefore, the surface distortion may not be serious for obtaining $\mathbf{r}_i^m$. However, it is worth mentioning that the details of the RCF are different from the ideally perfect crystal near the high-angle edge of the Bragg peak.

When the fluorescence absorption is very large, the main contribution to the RCF comes from the surface area. In this case, the remark made about $\mathbf{r}_a$ in the external SW method is equally applicable to $\mathbf{r}_i^m$, and the RCF is nearly the same as that expected in the external SW method. Fig. 6(*c*) shows a typical case.

In conclusion, the following procedures will be suggested for the accurate determination of foreign atoms by means of the SW methods. First of all, it is very desirable to measure the RC and the RCF accurately. If they show a small discrepancy between the observed and theoretical curves on the assumption of a perfect crystal, it is worth extending the crystal model to distorted crystals as has been done in this work. If the fitting is improved, one must abandon the conventional assumption.

Furthermore, to avoid an accidental coincidence between theory and experiments, it is suggested the experiments be performed for a few higher-order reflections as in the work of Hertel *et al.* (1985) or the experiments be carried out with different wavelengths. In the analysis, the parameters intrinsic to the host crystal should not be used as fitting parameters.

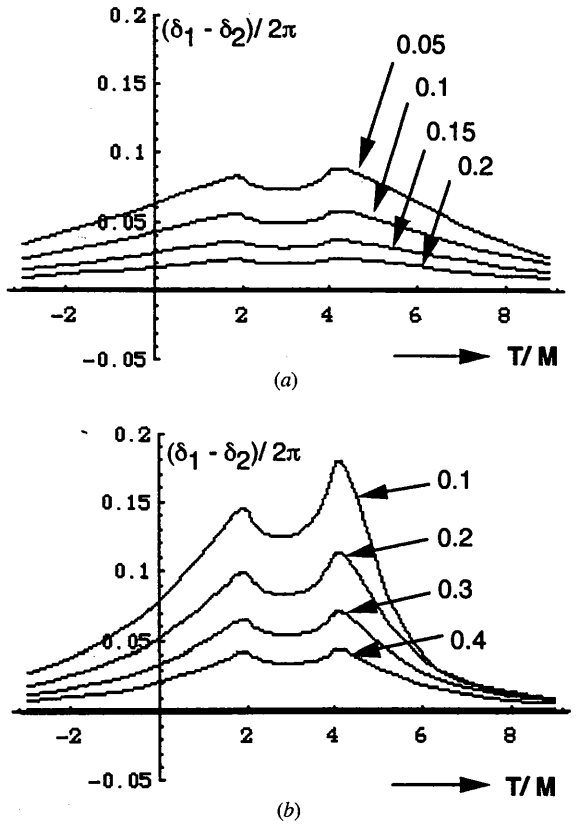

Fig. 7. The deviation of the phase angle δ from the perfect crystal. Absorption is assumed to be $A = 0.1$. The figures associated with arrow lines indicate $|\hat{x}_m|/\Lambda$, $\hat{x}_m$ being the net-plane position defined by equation (25). The bottom thick line corresponds to the bottom perfect crystal. (*a*) $H = 0.2$, (*b*) $H = 0.4$.

References

Abramowitz, M. & Stegun, L. A. (1964). *Handbook of Mathematical Functions*, Ch. 15. National Bureau of Standards, United States Department of Commerce, Washington, USA.

Anderson, S. K., Golovchenko, J. A. & Mair, G. (1976). *Phys. Rev. Lett.* **37**, 1141–1145.

Authier, A., Gronkowski, J. & Malgrange, C. (1989). *Acta Cryst.* A**45**, 432–441.

Bateman-Eredelyi, A. (1953). *Higher Transcendental Functions*, Vol. 1, Ch. 2. New York: McGraw-Hill.

Batterman, B. W. (1961). *Appl. Phys. Lett.* **1**, 68–69.

Batterman, B. W. (1964). *Phys. Rev. A*, **133**, 759–764.

Batterman, B. W. (1969). *Phys. Rev. Lett.* **22**, 703–705.

Bensoussan, S., Malgrange, C. & Sauvage-Simkin, M. (1987). *J. Appl. Cryst.* **20**, 222–229.

Golovchenko, J. A., Batterman, B. W. & Brown, L. (1974). *Phys. Rev. B*, **10**, 4239–4243.

Hertel, N., Materlik, G. & Zegenhagen, J. (1985). *Z. Phys.* B**58**, 199–204.

Kato, N. (1974). *X-ray Diffraction*, edited by L. V. Azároff. New York: McGraw-Hill.
Kato, N. (1990). *Acta Cryst.* A**46**, 672–681.
Kato, N. (1992*a*). *Acta Cryst.* A**48**, 829–834.
Kato, N. (1992*b*). *Acta Cryst.* A**48**, 834–841.
Kato, N. (1996). *X-ray and Neutron Dynamical Diffraction*, edited by A. Authier, S. Lagomarsino & B. K. Tanner, pp. 111–135. New York: Plenum.
Lagomarsino, S. (1996). *X-ray and Neutron Dynamical Diffraction*, edited by A. Authier, S. Lagomarsino & B. K. Tanner, pp. 225–234. New York: Plenum.
Patel, J. (1996). *X-ray and Neutron Dynamical Diffraction*, edited by A. Authier, S. Lagomarsino & B. K. Tanner, pp. 211–224. New York: Plenum.
Zachariasen, W. H. (1945). *Theory of X-ray Diffraction in Crystals*. New York: Wiley.